
PUSHING THE ENVELOPE FOR DEPTH-BASED SEMI-SUPERVISED 3D HAND POSE ESTIMATION WITH CONSISTENCY TRAINING

Mohammad Rezaei

Department of Computer Science and Engineering
University of Texas at Arlington
Arlington
mohammad.rezaei@mavs.uta.edu

Farnaz Farahanipad

Department of Computer Science and Engineering
University of Texas at Arlington
Arlington
farnaz.farahanipad@mavs.uta.edu

Alex Dillhoff

Department of Computer Science and Engineering
University of Texas at Arlington
Arlington
alex.dillhoff@uta.edu

Vassilis Athitsos

Department of Computer Science and Engineering
University of Texas at Arlington
Arlington
athitsos@uta.edu

ABSTRACT

Despite the significant progress that depth-based 3D hand pose estimation methods have made in recent years, they still require a large amount of labeled training data to achieve high accuracy. However, collecting such data is both costly and time-consuming. To tackle this issue, we propose a semi-supervised method to significantly reduce the dependence on labeled training data. The proposed method consists of two identical networks trained jointly: a teacher network and a student network. The teacher network is trained using both the available labeled and unlabeled samples. It leverages the unlabeled samples via a loss formulation that encourages estimation equivariance under a set of affine transformations. The student network is trained using the unlabeled samples with their pseudo-labels provided by the teacher network. For inference at test time, only the student network is used. Extensive experiments demonstrate that the proposed method outperforms the state-of-the-art semi-supervised methods by large margins.

Keywords Deep Learning, Computer Vision, 3D hand pose estimation

1 Introduction

The hands are the primary means by which humans interact with the outside world. As such, accurate hand pose estimation is a necessary requirement for many vision-based systems and enables many applications in areas such as augmented reality (AR), virtual reality (VR) and gesture recognition.

Recently, the availability of more accurate and affordable commodity depth cameras coupled with the success of Deep Neural Networks (DNN) has led to significant progress in depth-based 3D hand pose estimation and segmentation [1, 2, 3, 4, 5, 6, 7, 8, 9, 10]. Despite these advancements, one major challenge that remains is that DNN-based methods require large amounts of annotated training data to realize their full potential. A straightforward approach to mitigate this requirement is to use synthesized training data with accurate annotations [11], which can be generated with minimal human effort. However, models trained on synthesized data generalize poorly to the real-world data due to the significant domain gap between synthetic and real-world data. A popular alternative is semi-supervised learning (SSL) [12], where the goal is to leverage unlabeled data along with the labeled data, hence reducing the amount of labeled data required for training. Most of the recent advancements of SSL methods have been focused on image classification [13, 14, 15, 16, 17, 18, 19, 20, 21, 22, 23].

Semi-supervised learning has recently attracted attention in the area of 3D hand pose estimation. Chen et al. [3] leverage unlabeled data by minimizing the Chamfer loss between the input point cloud and its reconstructed version by a decoder. Wan et al. [24] jointly train two deep generative models with a shared latent space to model the statistical relationships of depth images and their corresponding hand poses. Their architectural design facilitates learning from unlabeled data. Poier et al. [11] exploit synthetic data to reduce reliance on annotated real-world data by learning to map from the features of real data to that of synthetic data. Baek et al. [8] synthesize data in the skeleton space and then its corresponding depth map to augment the training data. These methods enable semi-supervised learning through accommodations in their network architecture. Orthogonal to this line of work, we propose a model-agnostic semi-supervised framework for 3D hand pose estimation that takes advantage of the most recent advancements of SSL methods in image classification.

The proposed framework consists of two identical networks that are trained jointly: 1) student network and 2) teacher network. Any off-the-shelf network architecture can be used as long as it provides a means for prediction uncertainty estimation. For training the teacher, we adopt an approach based on consistency training [25]. Driven by the intuition that a good model should be robust to any small change in an input example, approaches based on the consistency training enforce the model predictions to be invariant to small noise applied to input examples. Inspired by this approach, we train the teacher network using both the labeled and unlabeled parts of the training data, with a combination of the typical supervised loss and an unsupervised loss formulated in such a way to enforce model consistency defined as the model output equivariance under a set of affine transformations.

Note that the proposed method uses different training strategies from [25] due to the fundamentally different nature of the 3D hand pose estimation, which is a structured regression task as opposed to an image classification task. This difference poses unique challenges for a hand pose estimation method based on consistency training, necessitating not only architectural changes but also different training strategies. We present several novel components to effectively address these challenges. The student network is trained using the pseudo-labels generated by the teacher network. More specifically, to stabilize the training, exponential moving average [26] of the teacher network’s parameters are used for generating the pseudo-labels. After the training is finished, the student network is fine-tuned on the labeled part of the training data since it has not seen any of them during training. Note that the proposed method comes at no additional cost at test time, as only the student network is used for inference and the teacher network is discarded after training.

It should be stressed that the proposed training of a separate student network is different from knowledge distillation [27]. The goal of knowledge distillation is to transfer the knowledge of a complicated model to a simpler model by training the simpler model with the softmax outputs of the complicated model. Moreover, knowledge distillation is performed after training. However, the proposed method employs two identical networks that are trained simultaneously. Furthermore, the student is trained using the exponential moving average (EMAN) of the teacher network’s parameters.

We conduct an extensive evaluation of the proposed method on three publicly available datasets, namely ICVL [28], MSRA [29] and NYU [9], which are challenging benchmarks commonly used for evaluation of 3D hand pose estimation methods. The results demonstrate that the proposed method significantly outperforms the current state-of-the-art semi-supervised hand pose estimation methods. We also analyse the performance of the proposed method in cases of severe scarcity of ground-truth annotations and show its effectiveness under such scenarios. Most remarkably, using only 25% of the annotations, the proposed method performs on par with the state-of-the-art fully supervised methods (methods that use 100% of the ground-truth annotations).

In summary, our contributions are as follows:

- We propose a novel semi-supervised hand pose estimation method to effectively leverage the unlabeled data. To the best of our knowledge, this is the first method to incorporate consistency training for semi-supervised training on depth images of hands.
- We propose several novel strategies to enable consistency training for 3D hand pose estimation on depth images.
- The proposed method is the first depth-based hand pose estimation method to incorporate advances from recent SSL methods such as [30, 25, 26], which target general-purpose image classification. A key contribution is proposing concrete ways to apply those ideas to depth-based hand pose estimation, and showing that they lead to improved performance.
- We empirically show that the proposed method outperforms the current state-of-the-art semi-supervised 3D hand pose estimation methods.

Code and models will be made publicly available upon acceptance.

2 Related Work

2.1 Hand Pose Estimation

Hand pose estimation has been a long-standing problem in the Computer Vision community. While early methods relied on non-data-driven approaches such as hand crafted features, optimization methods, and distance metrics [31, 32, 33], in recent years there has been a shift to methods based on deep neural networks (DNNs). While there have been many DNN-based methods proposed to perform 3D hand pose estimation from different data modalities, we keep our focus here on methods designed for depth images, as they are the most related to ours.

Oberweger et al. [34] proposed a method to estimate the hand pose represented by PCA coefficients of a statistical hand model. Wang et al. [35] use the ensemble principle by partitioning the last convolutional outputs of a CNN into several regions and using separate regressors to estimate the hand joints. Another line of work is to take advantage of the recent advancements in 3D Deep learning. To this end, [36, 37] converted 2.5D depth images into 3D voxels and employed 3D CNNs to estimate the 3D hand pose. Several methods [38, 6, 39, 3, 40, 41] have been recently proposed to utilize point cloud processing networks by converting depth images into point clouds as the input. Comprehensive reviews of depth-based hand pose estimation can be found in [42, 1].

The above-mentioned methods are all fully-supervised. Our work is most related to the recent line of semi-supervised methods for 3D hand pose estimation [3, 24, 11, 8]. SemiHand [43] is closest to our method. It uses consistency training, which is also the case for the proposed method. However, the consistency training approach in the proposed method is significantly different than that of [43]. Besides using a different input data modality (2.5 depth images as opposed to RGB images), the proposed framework is based on a student-teacher paradigm and uses consistency training only for training the teacher network, whereas SemiHand [43] uses a single network. The proposed framework also uses a fundamentally different mechanism for label-refinement and the network uncertainty estimation. Finally, unlike SemiHand [43], the proposed method only uses view consistency.

2.2 Semi-supervised Learning in Image Classification

The key challenge to training of modern DNNs is the requirement for large amounts of labeled data. Semi-supervised learning (SSL) mitigates this requirement by providing a means of leveraging unlabeled data. Classic examples of SSL methods include transductive models [13, 14, 15], entropy minimization [16], co-training [17, 18] and graph-based models [19, 20, 21, 22, 23].

Our work is closely related to the recent line of SSL methods based on pseudo-labeling [44, 45, 46], where they produce artificial label for unlabeled data samples and train the model to predict the artificial label when fed unlabeled samples as input, and consistency training [30, 25, 47] wherein they enforce the model predictions to be consistent across a sample and its perturbed version. However, the proposed method is fundamentally different from the methods discussed above. They are all focused on image classification, where the goal is encourage representation invariance across different views of the same image. However, the proposed method performs hand pose estimation, which is a structured regression task. It critically depends on spatial information and its goal is to enforce representation equivariance across different views. These differences pose unique challenges for a hand pose estimation method based on consistency training. In this paper, we propose several novel strategies to address these challenges and take advantage of the state-of-the-art SSL methods in image classification.

3 Proposed Method

3.1 Problem Formulation and Notation

The task of 3D hand pose estimation is defined as follows: given an input depth image $x \in \mathbb{R}^{H \times W}$, the task is to estimate the 3D location of a set of pre-defined hand joints $\mathcal{J} \in \mathbb{R}^{N_J \times 3}$ in the camera coordinate system by learning a mapping f in the form of a neural network parameterized by θ , such that $\mathcal{J} = f(X; \theta)$. H and W denote the height and width of the depth map respectively. For the sake of simplicity, we refer to the input data dimensionality as $d = H \times W$. We use N_J to refer to the number of estimated joints. $\mathcal{J}_i = (U, V, Z)$ represents the location of the i^{th} joint. The function f is learned using the training set consisting of labeled examples $(x_l, \mathcal{J}^l) \sim P_L$ and unlabeled examples $x_u \sim P_U$. P_l and P_U denote the probability distributions of labeled and unlabeled examples respectively. We define an augmentation function $\Phi : \mathbb{R}^d \rightarrow \mathbb{R}^d$ such that it maintains the equivariance property. This mathematically means that if $x' = \Phi(x)$, then we have $\mathcal{J}' = \Phi(\mathcal{J})$. We define \mathcal{M} as a uniform probability distribution over all such augmentation functions. In our experiments, we use a subset of affine transformations including translation, scaling and rotation as augmentation functions.

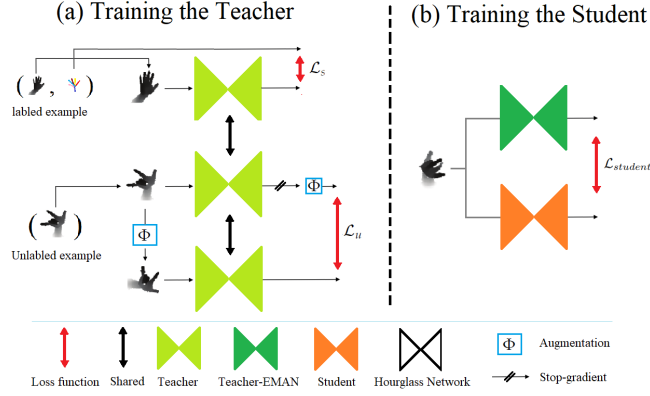


Figure 1: Left: overview of training the teacher network. It depicts a training batch consisting of one labeled example and one unlabeled example. The teacher network is trained using a combination of the typical supervised loss on the labeled examples and consistency loss on the unlabeled examples. Right: the student network is trained using the pseudo-labels provided by the EMAN of the teacher network’s parameters

The overview of the proposed method is illustrated in Fig. 1. It employs two identical networks called the teacher network and the student network, whose parameters are denoted by θ_T and θ_S respectively. The teacher network task is to provide supervisory signal for the student network by generating pseudo-labels. It is trained using a combination of the typical supervised loss and consistency training loss. As the teacher network improves, so do the pseudo-labels it generates for the student network. As a result, the student network keeps improving as the training of the teacher network progresses. After training is finished, the student network will be fine-tuned using the available labeled samples because it has not seen any of them during training. We empirically found that this leads to some modest performance improvements.

3.2 Network Architecture

Both the teacher and student network follow the same architecture that is similar to [48]. It consists of an encoder network and two separate branches. The encoder is a CNN whose task is to extract hand features from the input depth image. Its output feature volume serves as the input to two branches. The first branch estimates a heatmap H_j^{2D} for each joint. The 2D heatmap H_j^{2D} represents the occurrence likelihood of the j^{th} joint at each pixel location. The second branch estimates a depth map H_j^z for each joint. H_j^z represents depth prediction for the corresponding pixels for the j^{th} joint. The 3D locations are then computed following [49, 48]:

$$(U^j, V^j) = \sum_{u_i} \sum_{v_i} (u_i, v_i) \hat{H}_j^{2D}(u_i, v_i) \quad (1)$$

$$Z^j = \sum_{u_i} \sum_{v_i} H_j^z(u_i, v_i) \hat{H}_j^{2D}(u_i, v_i) \quad (2)$$

In the above, $\hat{H}_j^{2D}(u_i, v_i)$ is the H_j^{2D} normalized through spatial Softmax operation as follows:

$$\hat{H}_j^{2D}(x, y) = \frac{\exp(\alpha_j H_j^{2D}(x, y))}{\sum_{u_i, v_i \in \Omega} \exp(\alpha_j H_j^{2D}(u_i, v_i))} \quad (3)$$

Here, Ω represents the set of all pixel locations in the input map H_j^{2D} . α_j denotes the temperature parameter that controls the spread of the output heatmaps \hat{H}_j^{2D} . Unlike [48] that trains these parameters along with the rest of the network parameters, we set $\alpha_j = 1$ for $j \in 1, 2, \dots, N_j$ and keep them fixed during the training phase. In our experiments, we use an Hourglass network [50] as the encoder.

3.3 Teacher Network Training

The teacher network is trained using both labeled and unlabeled examples by solving the following optimization problem, conceptually similar to [25, 43]:

$$\begin{aligned} \min_{\theta_T} \mathcal{L}_s(\theta_T) + \lambda \mathcal{L}_u(\theta_T) = & \mathbb{E}_{(x_l, \mathcal{J}^l) \sim P_L(x)} [D(f(x_l; \theta_T), \mathcal{J}^l)] + \\ & \lambda \mathbb{E}_{x_u \sim P_U(x)} \mathbb{E}_{\Phi \sim \mathcal{M}} [D(\Phi(f(x_u; \bar{\theta}_T)), f(\Phi(x_u); \theta_T))] \end{aligned} \quad (4)$$

Here, D denotes mean element-wise L1 distance. $\bar{\theta}_T$ denotes a fixed copy of the current parameters θ_T , indicating the the gradient is not back-propagated through $\bar{\theta}_T$, as done in [25, 51]. λ is a weighting factor to balance the terms \mathcal{L}_s and \mathcal{L}_u . \mathcal{L}_s is the typical supervised loss computed on the labeled examples, which is aimed at minimizing the difference between the model predictions and the corresponding ground-truth labels. \mathcal{L}_u is the unsupervised consistency regularization loss computed on unlabeled examples to enforce consistency of the model predictions across different views of the same depth images. In contrast to image classification where the consistency is defined as the model prediction invariance across different views [25], we define consistency as equivariance under a set of affine transformations, similar to SemiHand [43]. Explicitly enforcing such an estimation equivariance on the unlabeled examples proves to be a very effective means of leveraging them. $f(x_u; \bar{\theta}_T)$ can be interpreted as the pseudo-labels generated by the teacher network from the view x_u to be used by its own in the second view $\Phi(x_u)$.

Sample Masking. Models trained using self-generated pseudo-labels generally suffer from confirmation bias [52], where the model keeps amplifying its own errors. It has been demonstrated that masking out noisy pseudo-labels and maintaining only high-quality ones for training can considerably reduce the confirmation bias [44]. The standard approach towards this end has been to base the decision of whether to use a pseudo-label for training on a model prediction certainty (or uncertainty) measure compared against a threshold. The typical approach in image classification, namely taking the maximum of the model output probability, is not applicable to the proposed method due to the different nature of its task. SemiHand [43] defined the model confidence on a data sample as the sum of the distance between the model’s prediction on an image and that of its randomly perturbed version, and the distance between the pseudo-label and its corrected pseudo-label. However, this approach requires additional model evaluations and performing forward kinematic chain, which adds computational overhead. The proposed method uses a simple yet effective method to measure the model uncertainty. The prediction uncertainty for the j^{th} joint, denoted by C_j , is approximated using the Standard deviation (STD) of the corresponding estimated normalized heatmap \hat{H}_j^{2D} , computed as follows:

$$C_j = \sqrt{\sum_{u_i} \sum_{v_i} \hat{H}_j^{2D}(u_i, v_i) \|[U_j, V_j]^T - [u_i, v_i]^T\|^2} \quad (5)$$

Here, $\|\cdot\|$ denotes the Frobenius norm function. We empirically found that when the model is certain about its prediction on a given joint, its corresponding heatmap has a low STD. On the other hand, when the model is not certain and there are many candidate pixels, the heatmap tends to be wider (and hence high STD).

We define the mask $M \in \mathbb{R}^J$ as follows:

$$M_j = \begin{cases} m_a & \text{if } C_j < T_j \\ m_r & \text{otherwise} \end{cases} \quad (6)$$

Here, T_j is the threshold used for masking the j^{th} joint. Symbols m_a and m_r denote the weights given to the pseudo-labels that are respectively accepted and rejected. Image classification SSL methods such as [30, 25, 53] have traditionally taken a binary approach for masking ($m_a = 1$ and $m_r = 0$), which is a special case of Eq. 6. While this binary approach has proven effective for image classification, we empirically found that including the pseudo-labels that are rejected in the training ($m_r \neq 0$) consistently leads to performance improvement in the proposed method. The L1 distance D in \mathcal{L}_u in the Eq. 4 is replaced by the following weighted average:

$$D(\mathcal{J}, \mathcal{J}') = \frac{1}{3K} \sum_{j=1}^{N_J} M_j \sum_{i=1}^3 |\mathcal{J}_{ji} - \mathcal{J}'_{ji}| \quad (7)$$

where $K = \sum_j M_j$. In the case where masking is not used, we set all $M_j = 1$.

Dynamic Thresholding. A standard practice of SSL methods in image classification is to use a fixed threshold for masking [30, 25]. Most recently, [53] employed a strategy for dynamic adjustment of thresholds for different classes based on class learning effects. However, none of these strategies is practical for the proposed method. Naively using fixed thresholds for masking causes two issues in the proposed method. First, since the uncertainty measure for different joints are of different scales (e.g. heatmaps corresponding to fingertips are usually very peaky but are relatively wide for the palm, leading to low and high STDs respectively), we would need N_j different thresholds (one for each joint), making the hyper-parameter optimization complicated. Secondly, adopting uncertainty-based pseudo-labeling leads to a class imbalance in the pseudo-labels, and thereby, misguides the training [54].

To tackle these issues, we employ a strategy to dynamically adjust the thresholds. Let ρ_t be the fraction of pseudo-labels allowed for training at the training epoch t . Let T_j^t be the threshold value used for masking for the j^{th} joint at the training epoch t . After initialization in the first epoch, T_j^{t+1} for the epoch $t + 1$ is computed as follows:

$$T_j^{t+1} = T_j^t + \eta(\rho_t - \rho_t^j) \quad (8)$$

Here, ρ_t^j is the fraction of pseudo-labels corresponding to the j^{th} joint accepted for training in the epoch t according to the corresponding threshold T_j^t . Symbol η denotes the adjustment rate. Intuitively, when $\rho_t > \rho_t^j$, it means that the threshold T_j^t should increase to let pass more pseudo-labels. On the other hand, when $\rho_t < \rho_t^j$, it means the threshold T_j^t should decrease to accept fewer pseudo-labels for training. This type of addressing class-imbalance problem can be thought of as equivalent to Mean Sampling [55]. It ensures that a roughly equal fraction ρ_t of pseudo-labels for each joint is used for training in each epoch. We use a cosine schedule strategy [56] to increase ρ_t from the initial value ρ_{start} to reach its final value ρ_{end} over the course of training as follows:

$$\rho_t = \rho_{start} + 0.5(1 - \cos(\frac{T_{cur}}{T_{max}}\pi))(\rho_{end} - \rho_{start}) \quad (9)$$

Here, T_{cur} and T_{max} denote the current epoch number and the total number of training epochs respectively. Intuitively, the proposed method allows only a small proportion of pseudo-labels to be used at early phases of the training since the teacher network is still not accurate in early training phases. As the training progresses and the teacher network performance improves, a larger proportion of pseudo-labels are allowed to be used for training.

3.4 Student Network Training

The proposed method trains the student network using the unlabeled samples and their corresponding pseudo-labels generated by the teacher network. However, using pseudo-labels generated directly by the teacher network can lead to a potential problem. The teacher itself is constantly updated in the training, which could cause performance degradation and training instability in the student network since it has to learn to approximate a highly non-stationary function. An alternative is to use the exponential moving average (EMA) of the teacher network’s parameters to generate pseudo-labels [52]. However, this approach could lead to a potential mismatch between the EMA parameters and the batch normalization (BN) statistics in the parameter space [26] because the EMA parameters are averaged from the previous iterations, but the batch-wise BN statistics are instantly collected at the current iteration. We use the recently proposed fix for this issue called EMAN [26], where the batch-wise statistics are exponentially averaged from the previous iterations as well. The student network is trained by solving the following optimization problem:

$$\min_{\theta_S} \mathcal{L}_{student} = \mathbb{E}_{x_u \sim P_U(x)} \mathbb{E}_{\Phi \sim \mathcal{M}} [D(f(\Phi(x_u); \theta_{EMAN}), f(\Phi(x_u); \theta_S))] \quad (10)$$

where θ_{EMAN} denotes the exponentially moving averaged of the teacher network’s parameters from the previous iterations computed as in [26]. $f(\Phi(x_u); \theta_{EMAN})$ are the pseudo-labels corresponding to x_u generated using EMAN parameters.

4 Experiments

4.1 Implementation Details

The input to the networks is prepared by cropping the hand area from a depth image following [57] and resizing it to a fixed size of 128x128. The depth values are then normalized to [-1, 1] for the cropped image. For training, we use Adam [58] optimizer with a cosine learning rate decay schedule [56]. The initial learning rate is set to be 10^{-4} , and a weight decay of 10^{-5} is used. The augmentation set used for \mathcal{M} includes in-plane rotation ([-180, 180] degree), 3D scaling ([0.9, 1.1]), and 3D translation ([-10, 10] mm). The proposed method uses diffident combinations of hyper parameters depending on the extent of the availability of the ground-truth labels. We refer the reader to the supplementary material for more details. We use PyTorch framework [59] for implementation.

Table 1: Performance under different strategies for adjusting the thresholds

Strategy	Error (mm)
Fixed Thresholds	10.43
$\rho_t = 0.4$	9.00
$\rho_t = 0.6$	8.84
$\rho_t = 0.8$	8.99
Ours	8.71

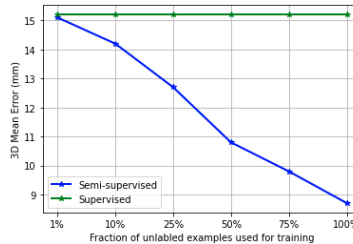


Figure 2: The performance of the model under different percentages of unlabeled examples used for training

4.2 Datasets and Evaluation Metrics

We evaluate the proposed method on three public 3D hand pose estimation datasets: ICVL dataset [28], NYU dataset [9] and MSRA dataset [29]. The ICVL dataset contains 22K training and 1.5K testing depth images that are captured with an Intel Realsense camera. The ground truth hand pose of each image consists of $N_j = 16$ joints. The NYU dataset is captured with three Microsoft Kinects from different views. Each view consists of 72K training and 8K testing depth images. Following most previous works, we only use the frontal view and use a subset $N_j = 14$ out of the total 36 annotated joints for training and testing in all experiments. The MSRA dataset [29] contains more than 76K frames captured from 9 subjects. Each subject contains 17 hand gestures and each hand gesture has about 500 frames. Each frame is provided with a ground-truth of $N_j = 21$ joints. Following the protocol used by [29], we evaluate the proposed method on this dataset with the leave-one-subject-out cross-validation strategy.

For evaluation, we use one of the most commonly used metrics for evaluating 3D hand pose estimation methods: the mean distance error (measured in mm). The mean distance error represents the average Euclidean distance between the estimated and the ground-truth joint locations computed over the entire testing set.

4.3 Ablation Study

To conduct ablation study, we choose a scenario where labeled data is scarce (more specifically, 1% of the ground-truth labels are used) because such a scenario most highlights the proposed method’s capability to leverage the unlabeled data. We use the NYU dataset for performing ablation study.

Impact of Sample Masking. We study the impact of using sample masking in the training. First, we use the ground-truth labels of the unlabeled data to illustrate how the accuracy of pseudo-labels improves when we use heatmap *STDs* as the uncertainty measure to mask out noisy pseudo-labels. As shown in Fig. 3, this approach leads to a consistent improvement of between 10% to 25% in the accuracy of pseudo-labels. As can be seen in Table 3, incorporating the proposed sample masking significantly improves the performance.

Effectiveness of Dynamic Thresholding. We examine the effectiveness of the the proposed dynamic thresholding strategy in our framework. We report the performance in three cases. In the first case, the thresholds are initialized and then kept fixed during training. The second case includes scenarios where the thresholds are dynamically adjusted according to Eq. 8, but ρ_t is kept fixed. The third case refers to the proposed strategy, where ρ_t is adjusted according to a cosine schedule [56]. As can be seen in Table 1, the proposed strategy leads to the best performing case.

Impact of Using a Separate Network as the Student. Empirical evidence demonstrate that using a separate network as the student (as opposed to using a single network as both the teacher and the student) leads to a performance improvement of 0.59 mm. We conjecture that this improvement primarily stems from the fact the the student network is trained using a more stationary data distribution (only the pairs of unlabeled examples and their pseudo-labels provided by the EMAN of the teacher network’s parameters), as opposed to the teacher network that is trained using a

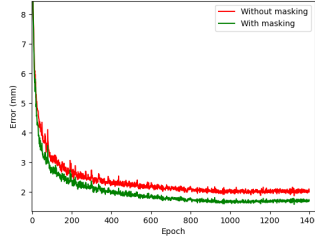


Figure 3: The accuracy of pseudo-labels generated by the teacher network with and without applying masking

Table 2: Parameters used for generating pseudo-labels for training the student

Model Parameters	Error (mm)
Teacher	9.27
EMA-Teacher	10.28
EMAN-Teacher	8.71

combination of distributions (pairs of labeled examples and their ground-truth labels and pairs of unlabeled examples and their corresponding pseudo-labels).

Impact of Using EMAN for Generating Pseudo-Labels. To analyse the impact of using EMAN of the teacher network’s parameters (instead of the parameters themselves) for generating the training pseudo-labels for the student network, we compare the performance of the student network in three cases in terms of the parameters used for generating pseudo-labels for its training: 1) the teacher network’s parameters, 2) EMA-teacher [52] and 3) EMAN-teacher [26]. As can be seen in Table 2, the best performing case is when we use EMAN. EMAN greatly improves the stability of learning by constraining the target values for the student network to change more slowly.

4.4 Ability To Leverage Unlabeled Examples

We analyze the effectiveness of the proposed method in leveraging unlabeled data, which is the key ability a semi-supervised method is aimed at achieving. Specifically, we use 1% of the dataset as the labeled portion of the training data, and gradually expand the unlabeled portion of the training data. As can be seen in Fig. 2, as the number of unlabeled data samples increases, the performance consistently improves. This clearly demonstrates the high capability of the proposed method of leveraging the unlabeled examples to improve its performance.

4.5 Comparison with State-of-the-Art Semi-Supervised Hand Pose Estimation Methods

To demonstrate the effectiveness of the proposed method, we compare it with the state-of-the-art depth-based semi-supervised methods including [3, 24, 8, 60]. Note that Beak et al. [8] particularly adopt a different approach from the rest of the works. They synthesize data in the skeleton space and train a separate network to synthesize its corresponding depth image. Although they use 100% of training data annotations, we include their work in our comparison as it is aimed at the same goal as the rest of the works. As can be seen in Table 4, the proposed method significantly outperforms the state-of-the-art methods. Most notably, the proposed method surpasses all the existing methods when only using 1% of ground-truth annotations for training.

The results from Table 4 also show that the proposed method enjoys a high label efficiency. Specifically, the performance of the proposed method reaches its highest level when using only 25% of the ground-truth annotations. It does not achieve a considerable performance gain when more ground-truth annotations are used. Interestingly, the performance gap between the cases where 1% and 100% of the ground-truth annotations are used is only 0.7 mm. These observations clearly demonstrate the high capability of the proposed method of taking full advantage of the unlabeled examples. On the other hand, the existing methods rely more on the labeled data. For example, for SO-HandNet [3], the performance gap between the cases where 25% and 100% of the ground-truth annotations are used is 3.7 mm and 3.4 mm on NYU and ICVL respectively, indicating a very lower label efficiency.

4.6 Semi-Supervised Learning under Extremely Low Data Regimes

We compare the proposed method with MURAUER [11], which to the best of our knowledge is the only depth-based 3D hand pose estimation method examined under scenarios of severe labeled data scarcity. As can be seen in Table 5,

Table 3: Impact of different masking approaches on the performance

Masking Approach	Error (mm)
No masking	9.79
Binary-masking	9.12
Ours	8.71

Table 4: Comparison of the proposed method with state-of-the-art semi-supervised methods on ICVL and NYU datasets. The performance is evaluated by the test estimation error under different percentages of labeled data used for model training

Method	Label Usage	Augmented Set	ICVL(mm)	NYU(mm)
Beak et al.(baseline)	100%	No	12.10	17.30
Beak et al.(w/o aug.; refine)	100%	No	10.40	16.40
Beak et al.(w/o refine)	100%	Yes, 10 times	9.10	14.90
Beak et al.	100%	Yes, 10 times	8.50	14.10
LSPS [60]	25%	No	7.35	15.70
	50%	No	7.10	15.45
	75%	No	7.05	15.45
	100%	No	7.00	15.40
Crossing Net [24]	25%	No	10.50	16.10
	50%	No	10.0	16.0
	75%	No	10.10	15.90
	100%	No	10.20	15.50
SO-HandNet [3]	25%	No	11.10	14.90
	50%	No	9.40	14.10
	75%	No	9.10	12.80
	100%	No	7.70	11.20
Ours	25%	No	6.11	8.14
	50%	No	6.06	8.11
	75%	No	6.04	8.06
	100%	No	5.99	8.01
Ours	1%	No	6.94	8.71

the proposed method significantly outperforms MURAUER [11] under the three out of the four scenarios. The only scenario where the proposed method is inferior is when there are only 10 labeled examples. This is because such a small amount of labeled training data lacks adequate information about the nature of the task. MURAUER [11] compensates for this lack of information by pre-training on synthetic data. However, the proposed method does not use any pre-training. More importantly, in contrast to MURAUER [11], the proposed method achieves this performance without the application-limiting requirement for multi-view real-data. Remarkably, in the case where there are only 100 labeled samples, the proposed method achieves 12.11 mm, which clearly demonstrates the practicality of the proposed method in cases of severely limited access to labeled data.

4.7 Comparison with State-of-the-Art Fully-Supervised Methods

We compare the proposed method with state-of-the-art methods that use 100% of ground-truth annotations for training [61, 34, 57, 62, 35, 65, 66, 7, 5, 4, 64, 36, 63, 38, 6, 41, 40, 37]. Table 6 summarizes the performance based on the mean distance error on the three datasets. As can be seen in Table 6, despite using only 25% of the ground-truth annotations, the proposed method ranks as the best performing method on the NYU dataset, the second best performing

Table 5: Comparison of our work with [11] under cases of severely limited access to labels on the NYU dataset. Numbers next to the methods represent their performance under the corresponding scenarios in terms of mean distance error in mm

Methods	Number of Labeled Examples			
	10	100	1,000	10,000
MURAUER [11]	16.4	12.2	10.90	9.90
Ours	25.82	12.11	8.60	8.16

Table 6: Comparison with the state-of-the-art fully-supervised methods on ICVL [28] (Left), NYU [9] (Middle), and MSRA [29] (Right). “Error” indicates the mean distance error in mm. 25p and 100p respectively denote the cases where 25% and 100% of the ground-truth annotations are used for training

Methods	Error	Methods	Error	Methods	Error
DeepModel [61]	11.56	DeepPrior [34]	19.73	REN-9x6x6 [35]	9.79
DeepPrior [34]	10.40	DeepModel [61]	17.04	3DCNN [36]	9.58
DeepPrior++ [57]	8.10	3DCNN [36]	14.10	DeepPrior++ [57]	9.5
REN-4x6x6 [62]	7.63	REN-4x6x6 [62]	13.39	Pose-REN [65]	8.65
REN-9x6x6 [35]	7.31	REN-9x6x6 [35]	12.69	HandPointNet [38]	8.5
DenseReg [7]	7.30	DeepPrior++ [57]	12.24	CrossInfoNet [4]	7.86
SHPR-Net [63]	7.22	Pose-REN [65]	11.81	SHPR-Net [63]	7.76
HandPointNet [38]	6.94	Generalized-Feedback [66]	10.89	Point-to-Point [6]	7.7
CrossInfoNet [4]	6.73	HandPointNet [38]	10.54	V2V-PoseNet [37]	7.59
NARHT [41]	6.47	DenseReg [7]	10.20	JGR-P2O [64]	7.55
A2J [5]	6.46	CrossInfoNet [4]	10.08	NARHT [41]	7.55
Point-to-Point [6]	6.30	NARHT [41]	9.80	HandFoldingNet [40]	7.34
V2V-PoseNet [37]	6.28	Point-to-Point [6]	9.10	DenseReg [7]	7.23
JGR-P2O [64]	6.02	A2J [5]	8.61	Ours-25p	7.28
HandFoldingNet [40]	5.95	HandFoldingNet [40]	8.58	Ours-100p	7.18
Ours-25p	6.11	V2V-PoseNet [37]	8.42		
Ours-100p	5.99	JGR-P2O [64]	8.29		
		Ours-25p	8.14		
		Ours-100p	8.01		

on the MSRA dataset, and the third best performing on the ICVL dataset. These observations clearly demonstrate the success of the proposed framework in significantly reducing the reliance on the labeled training data.

5 Conclusion

In this paper, we propose a novel framework for performing depth-based 3D hand pose estimation under scenarios where the access to the labeled data is limited. The proposed framework consists of two identical networks that are jointly trained. The teacher network is trained using consistency training on both labeled and unlabeled examples by adapting some of latest advancements in SSL methods in image classification. The student network is trained using the unlabeled examples and their corresponding pseudo-labels provided by the teacher network. Extensive experiments demonstrate the proposed framework outperforms the current state-of-the-art methods by large margins.

References

- [1] Shanxin Yuan, Guillermo Garcia-Hernando, Björn Stenger, Gyeongsik Moon, Ju Yong Chang, Kyoung Mu Lee, Pavlo Molchanov, Jan Kautz, Sina Honari, Lihao Ge, et al. Depth-based 3d hand pose estimation: From current achievements to future goals. In *Proceedings of the IEEE Conference on Computer Vision and Pattern Recognition*, pages 2636–2645, 2018.
- [2] Jameel Malik, Ibrahim Abdelaziz, Ahmed Elhayek, Soshi Shimada, Sk Aziz Ali, Vladislav Golyanik, Christian Theobalt, and Didier Stricker. Handvoxnnet: Deep voxel-based network for 3d hand shape and pose estimation from a single depth map. In *Proceedings of the IEEE/CVF Conference on Computer Vision and Pattern Recognition*, pages 7113–7122, 2020.
- [3] Yujin Chen, Zhigang Tu, Lihao Ge, Dejun Zhang, Ruizhi Chen, and Junsong Yuan. So-handnet: Self-organizing network for 3d hand pose estimation with semi-supervised learning. In *Proceedings of the IEEE International Conference on Computer Vision*, pages 6961–6970, 2019.
- [4] Kuo Du, Xiangbo Lin, Yi Sun, and Xiaohong Ma. CrossinfoNet: Multi-task information sharing based hand pose estimation. In *Proceedings of the IEEE Conference on Computer Vision and Pattern Recognition*, pages 9896–9905, 2019.

- [5] Fu Xiong, Boshen Zhang, Yang Xiao, Zhiguo Cao, Taidong Yu, Joey Tianyi Zhou, and Junsong Yuan. A2j: Anchor-to-joint regression network for 3d articulated pose estimation from a single depth image. In *Proceedings of the IEEE International Conference on Computer Vision*, pages 793–802, 2019.
- [6] Lihao Ge, Zhou Ren, and Junsong Yuan. Point-to-point regression pointnet for 3d hand pose estimation. In *Proceedings of the European conference on computer vision (ECCV)*, pages 475–491, 2018.
- [7] Chengde Wan, Thomas Probst, Luc Van Gool, and Angela Yao. Dense 3d regression for hand pose estimation. In *Proceedings of the IEEE Conference on Computer Vision and Pattern Recognition*, pages 5147–5156, 2018.
- [8] Seungryul Baek, Kwang In Kim, and Tae-Kyun Kim. Augmented skeleton space transfer for depth-based hand pose estimation. In *Proceedings of the IEEE Conference on Computer Vision and Pattern Recognition*, pages 8330–8339, 2018.
- [9] Jonathan Tompson, Murphy Stein, Yann Lecun, and Ken Perlin. Real-time continuous pose recovery of human hands using convolutional networks. *ACM Transactions on Graphics (ToG)*, 33(5):1–10, 2014.
- [10] Abhishake Kumar Bojja, Franziska Mueller, Sri Raghu Malireddi, Markus Oberweger, Vincent Lepetit, Christian Theobalt, Kwang Moo Yi, and Andrea Tagliasacchi. Handseg: An automatically labeled dataset for hand segmentation from depth images. In *2019 16th Conference on Computer and Robot Vision (CRV)*, pages 151–158. IEEE, 2019.
- [11] Georg Poier, Michael Opitz, David Schinagl, and Horst Bischof. Murauer: Mapping unlabeled real data for label austerity. In *2019 IEEE Winter Conference on Applications of Computer Vision (WACV)*, pages 1393–1402. IEEE, 2019.
- [12] Olivier Chapelle, Bernhard Scholkopf, and Alexander Zien. Semi-supervised learning (chapelle, o. et al., eds.; 2006)[book reviews]. *IEEE Transactions on Neural Networks*, 20(3):542–542, 2009.
- [13] Ayhan Demiriz, Kristin P Bennett, and Mark J Embrechts. Semi-supervised clustering using genetic algorithms. *Artificial neural networks in engineering (ANNIE-99)*, pages 809–814, 1999.
- [14] Alex Gammerman, Volodya Vovk, and Vladimir Vapnik. Learning by transduction. *arXiv preprint arXiv:1301.7375*, 2013.
- [15] Thorsten Joachims et al. Transductive inference for text classification using support vector machines. In *Icml*, volume 99, pages 200–209, 1999.
- [16] Yves Grandvalet, Yoshua Bengio, et al. Semi-supervised learning by entropy minimization. *CAP*, 367:281–296, 2005.
- [17] Avrim Blum and Tom Mitchell. Combining labeled and unlabeled data with co-training. In *Proceedings of the eleventh annual conference on Computational learning theory*, pages 92–100, 1998.
- [18] Kamal Nigam and Rayid Ghani. Analyzing the effectiveness and applicability of co-training. In *Proceedings of the ninth international conference on Information and knowledge management*, pages 86–93, 2000.
- [19] Mikhail Belkin, Irina Matveeva, and Partha Niyogi. Regularization and semi-supervised learning on large graphs. In *International Conference on Computational Learning Theory*, pages 624–638. Springer, 2004.
- [20] Avrim Blum and Shuchi Chawla. Learning from labeled and unlabeled data using graph mincuts. 2001.
- [21] Yihui He, Ji Lin, Zhijian Liu, Hanrui Wang, Li-Jia Li, and Song Han. Amc: Automl for model compression and acceleration on mobile devices. In *Proceedings of the European conference on computer vision (ECCV)*, pages 784–800, 2018.
- [22] Fei Wang and Changshui Zhang. Label propagation through linear neighborhoods. *IEEE Transactions on Knowledge and Data Engineering*, 20(1):55–67, 2007.
- [23] Junnan Li, Caiming Xiong, and Steven CH Hoi. Comatch: Semi-supervised learning with contrastive graph regularization. In *Proceedings of the IEEE/CVF International Conference on Computer Vision*, pages 9475–9484, 2021.
- [24] Chengde Wan, Thomas Probst, Luc Van Gool, and Angela Yao. Crossing nets: Combining gans and vaes with a shared latent space for hand pose estimation. In *Proceedings of the IEEE Conference on Computer Vision and Pattern Recognition*, pages 680–689, 2017.
- [25] Qizhe Xie, Zihang Dai, Eduard Hovy, Minh-Thang Luong, and Quoc V Le. Unsupervised data augmentation for consistency training. *arXiv preprint arXiv:1904.12848*, 2019.
- [26] Zhaowei Cai, Avinash Ravichandran, Subhansu Maji, Charless Fowlkes, Zhuowen Tu, and Stefano Soatto. Exponential moving average normalization for self-supervised and semi-supervised learning. In *Proceedings of the IEEE/CVF Conference on Computer Vision and Pattern Recognition*, pages 194–203, 2021.

- [27] Geoffrey Hinton, Oriol Vinyals, and Jeff Dean. Distilling the knowledge in a neural network. *arXiv preprint arXiv:1503.02531*, 2015.
- [28] Danhang Tang, Hyung Jin Chang, Alykhan Tejani, and Tae-Kyun Kim. Latent regression forest: Structured estimation of 3d articulated hand posture. In *Proceedings of the IEEE conference on computer vision and pattern recognition*, pages 3786–3793, 2014.
- [29] Xiao Sun, Yichen Wei, Shuang Liang, Xiaoou Tang, and Jian Sun. Cascaded hand pose regression. In *Proceedings of the IEEE conference on computer vision and pattern recognition*, pages 824–832, 2015.
- [30] Kihyuk Sohn, David Berthelot, Chun-Liang Li, Zizhao Zhang, Nicholas Carlini, Ekin D Cubuk, Alex Kurakin, Han Zhang, and Colin Raffel. Fixmatch: Simplifying semi-supervised learning with consistency and confidence. *arXiv preprint arXiv:2001.07685*, 2020.
- [31] Vassilis Athitsos and Stan Sclaroff. Estimating 3d hand pose from a cluttered image. In *2003 IEEE Computer Society Conference on Computer Vision and Pattern Recognition, 2003. Proceedings.*, volume 2, pages II–432. IEEE, 2003.
- [32] Toby Sharp, Cem Keskin, Duncan Robertson, Jonathan Taylor, Jamie Shotton, David Kim, Christoph Rhemann, Ido Leichter, Alon Vinnikov, Yichen Wei, et al. Accurate, robust, and flexible real-time hand tracking. In *Proceedings of the 33rd Annual ACM Conference on Human Factors in Computing Systems*, pages 3633–3642, 2015.
- [33] Iason Oikonomidis, Nikolaos Kyriazis, and Antonis A Argyros. Efficient model-based 3d tracking of hand articulations using kinect. In *BmVC*, volume 1, page 3, 2011.
- [34] Markus Oberweger, Paul Wohlhart, and Vincent Lepetit. Hands deep in deep learning for hand pose estimation. *arXiv preprint arXiv:1502.06807*, 2015.
- [35] Guijin Wang, Xinghao Chen, Hengkai Guo, and Cairong Zhang. Region ensemble network: Towards good practices for deep 3d hand pose estimation. *Journal of Visual Communication and Image Representation*, 55:404–414, 2018.
- [36] Lihao Ge, Hui Liang, Junsong Yuan, and Daniel Thalmann. 3d convolutional neural networks for efficient and robust hand pose estimation from single depth images. In *Proceedings of the IEEE Conference on Computer Vision and Pattern Recognition*, pages 1991–2000, 2017.
- [37] Gyeongsik Moon, Ju Yong Chang, and Kyoung Mu Lee. V2v-posenet: Voxel-to-voxel prediction network for accurate 3d hand and human pose estimation from a single depth map. In *Proceedings of the IEEE conference on computer vision and pattern recognition*, pages 5079–5088, 2018.
- [38] Lihao Ge, Yujun Cai, Junwu Weng, and Junsong Yuan. Hand pointnet: 3d hand pose estimation using point sets. In *Proceedings of the IEEE Conference on Computer Vision and Pattern Recognition*, pages 8417–8426, 2018.
- [39] Shile Li and Dongheui Lee. Point-to-pose voting based hand pose estimation using residual permutation equivariant layer. In *Proceedings of the IEEE/CVF Conference on Computer Vision and Pattern Recognition*, pages 11927–11936, 2019.
- [40] Wencan Cheng, Jae Hyun Park, and Jong Hwan Ko. Handfoldingnet: A 3d hand pose estimation network using multiscale-feature guided folding of a 2d hand skeleton. In *Proceedings of the IEEE/CVF International Conference on Computer Vision*, pages 11260–11269, 2021.
- [41] Lin Huang, Jianchao Tan, Ji Liu, and Junsong Yuan. Hand-transformer: non-autoregressive structured modeling for 3d hand pose estimation. In *European Conference on Computer Vision*, pages 17–33. Springer, 2020.
- [42] James S Supancic, Grégory Rogez, Yi Yang, Jamie Shotton, and Deva Ramanan. Depth-based hand pose estimation: data, methods, and challenges. In *Proceedings of the IEEE international conference on computer vision*, pages 1868–1876, 2015.
- [43] Linlin Yang, Shicheng Chen, and Angela Yao. Semihand: Semi-supervised hand pose estimation with consistency. In *Proceedings of the IEEE/CVF International Conference on Computer Vision*, pages 11364–11373, 2021.
- [44] Eric Arazo, Diego Ortego, Paul Albert, Noel E O’Connor, and Kevin McGuinness. Pseudo-labeling and confirmation bias in deep semi-supervised learning. In *2020 International Joint Conference on Neural Networks (IJCNN)*, pages 1–8. IEEE, 2020.
- [45] Jiangfan Han, Ping Luo, and Xiaogang Wang. Deep self-learning from noisy labels. In *Proceedings of the IEEE/CVF International Conference on Computer Vision*, pages 5138–5147, 2019.
- [46] Paola Cascante-Bonilla, Fuwen Tan, Yanjun Qi, and Vicente Ordonez. Curriculum labeling: Revisiting pseudo-labeling for semi-supervised learning. *arXiv preprint arXiv:2001.06001*, 2020.

- [47] Chengyue Gong, Dilin Wang, and Qiang Liu. Alphamatch: Improving consistency for semi-supervised learning with alpha-divergence. In *Proceedings of the IEEE/CVF Conference on Computer Vision and Pattern Recognition*, pages 13683–13692, 2021.
- [48] Umar Iqbal, Pavlo Molchanov, Thomas Breuel Juergen Gall, and Jan Kautz. Hand pose estimation via latent 2.5 d heatmap regression. In *Proceedings of the European Conference on Computer Vision (ECCV)*, pages 118–134, 2018.
- [49] Xiao Sun, Bin Xiao, Fangyin Wei, Shuang Liang, and Yichen Wei. Integral human pose regression. In *Proceedings of the European Conference on Computer Vision (ECCV)*, pages 529–545, 2018.
- [50] Alejandro Newell, Kaiyu Yang, and Jia Deng. Stacked hourglass networks for human pose estimation. In *European conference on computer vision*, pages 483–499. Springer, 2016.
- [51] Takeru Miyato, Shin-ichi Maeda, Masanori Koyama, and Shin Ishii. Virtual adversarial training: a regularization method for supervised and semi-supervised learning. *IEEE transactions on pattern analysis and machine intelligence*, 41(8):1979–1993, 2018.
- [52] Antti Tarvainen and Harri Valpola. Mean teachers are better role models: Weight-averaged consistency targets improve semi-supervised deep learning results. *arXiv preprint arXiv:1703.01780*, 2017.
- [53] Bowen Zhang, Yidong Wang, Wenxin Hou, Hao Wu, Jindong Wang, Manabu Okumura, and Takahiro Shinozaki. Flexmatch: Boosting semi-supervised learning with curriculum pseudo labeling. *Advances in Neural Information Processing Systems*, 34, 2021.
- [54] Islam Nassar, Samitha Herath, Ehsan Abbasnejad, Wray Buntine, and Gholamreza Haffari. All labels are not created equal: Enhancing semi-supervision via label grouping and co-training. In *Proceedings of the IEEE/CVF Conference on Computer Vision and Pattern Recognition*, pages 7241–7250, 2021.
- [55] Ju He, Adam Kortylewski, Shaokang Yang, Shuai Liu, Cheng Yang, Changhu Wang, and Alan Yuille. Rethinking re-sampling in imbalanced semi-supervised learning. *arXiv preprint arXiv:2106.00209*, 2021.
- [56] Ilya Loshchilov and Frank Hutter. Sgdr: Stochastic gradient descent with warm restarts. *arXiv preprint arXiv:1608.03983*, 2016.
- [57] Markus Oberweger and Vincent Lepetit. Deeprior++: Improving fast and accurate 3d hand pose estimation. In *Proceedings of the IEEE international conference on computer vision Workshops*, pages 585–594, 2017.
- [58] Diederik P Kingma and Jimmy Ba. Adam: A method for stochastic optimization. *arXiv preprint arXiv:1412.6980*, 2014.
- [59] Adam Paszke, Sam Gross, Francisco Massa, Adam Lerer, James Bradbury, Gregory Chanan, Trevor Killeen, Zeming Lin, Natalia Gimelshein, Luca Antiga, et al. Pytorch: An imperative style, high-performance deep learning library. *Advances in neural information processing systems*, 32:8026–8037, 2019.
- [60] Masoud Abdi, Ehsan Abbasnejad, Chee Peng Lim, and Saeid Nahavandi. 3d hand pose estimation using simulation and partial-supervision with a shared latent space. *arXiv preprint arXiv:1807.05380*, 2018.
- [61] Xingyi Zhou, Qingfu Wan, Wei Zhang, Xiangyang Xue, and Yichen Wei. Model-based deep hand pose estimation. *arXiv preprint arXiv:1606.06854*, 2016.
- [62] Hengkai Guo, Guijin Wang, Xinghao Chen, Cairong Zhang, Fei Qiao, and Huazhong Yang. Region ensemble network: Improving convolutional network for hand pose estimation. In *2017 IEEE International Conference on Image Processing (ICIP)*, pages 4512–4516. IEEE, 2017.
- [63] Xinghao Chen, Guijin Wang, Cairong Zhang, Tae-Kyun Kim, and Xiangyang Ji. Shpr-net: Deep semantic hand pose regression from point clouds. *IEEE Access*, 6:43425–43439, 2018.
- [64] Linpu Fang, Xingyan Liu, Li Liu, Hang Xu, and Wenxiong Kang. Jgr-p2o: joint graph reasoning based pixel-to-offset prediction network for 3d hand pose estimation from a single depth image. In *European Conference on Computer Vision*, pages 120–137. Springer, 2020.
- [65] Xinghao Chen, Guijin Wang, Hengkai Guo, and Cairong Zhang. Pose guided structured region ensemble network for cascaded hand pose estimation. *Neurocomputing*, 395:138–149, 2020.
- [66] Markus Oberweger, Paul Wohlhart, and Vincent Lepetit. Generalized feedback loop for joint hand-object pose estimation. *IEEE transactions on pattern analysis and machine intelligence*, 42(8):1898–1912, 2019.